PREDICTION OF TRANSIENT DEFORMATION BY COUPLING CFD AND FEM ANALYSIS USING MACHINE LEARNING BASED CORRELATION FUNCTION

Jan Pařez, Patrik Kovář & Tomáš Vampola

Center of Aviation and Space Research, Czech Technical University in Prague.
Jugoslávských partyzánů 1580/3, 160 00 Prague, Czech Republic

Abstract

Determining transient deformation, considering the influence of fluid flow, is currently a very computationally demanding method. The paper discusses the study of numerical method for coupling between CFD and FEM in heat transfer for transient analysis of aero engines applications.

Keywords: CFD and FEM Coupling; 3D FEM Model; Rotor Thermal Bow; Natural Convection

1. Introduction

A key aspect of modern aircraft engine development involves effectively cooling highly heat-stressed engine parts. The longevity of these components, and consequently the entire engine, heavily relies on material temperatures. This necessitates accurately predicting material temperatures under specific operational conditions. Conjugated Heat Transfer (CHT), initially formulated by Perelman [1], delves into the interaction between solid components and fluids. Flow dynamics have a pivotal role in influencing material temperatures and thermal exchanges, leading to secondary flow within compressors' and turbines' concentric annular spaces. Optimizing the design requires considering transient processes, solid-fluid interactions, and the disparity in thermal behavior between the solid and the fluid.

In analyzing temperature and stress distributions within compressor or turbine components over time, the Finite Element Method (FEM) is commonly used. Material thermal loads resulting from these analyses are often described by simplified boundary condition models derived from empirical correlations, such as the advective one-dimensional models introduced by Fiedler et al. [2]. Research by Heselhaus and Vogel [3] shows that using simulations considering three-dimensional effects in transient conjugate flow and heat transfer significantly enhances accuracy without relying on empirical correlations. Conversely, inadequate modeling of transient changes during flight can lead to critical clearances or thermal stresses, as highlighted by Sun et al. [4]. However, performing conjugate simulations for the entire mission while accounting for different time scales becomes prohibitively computationally intensive due to the vastly differing heat transfer rates between fluids and solids.

To address computational complexity, Sun et al. [4] introduced weak coupling methods involving optimized programs independently simulating heat transfer in fluids and solids. This approach allows to use of a FEM code to compute the solid's thermal behavior while employing computational fluid dynamics (CFD) to model the adjacent flow. Achieving a physically accurate and stable solution in this coupled system requires information exchange between the FEM and CFD codes via a shared interface. Various strategies detailed in the literature exist for this purpose.

Errera and Duchaine [5] explored different coupling coefficients and continuity of exchange variables, based on the Dirichlet-Robin transfer procedure for stable and rapid convergence, contingent upon satisfying specific interface-based criteria. Gimenez et al. [6] proposed approaches for updating boundary conditions between coupling points, favoring the quasi-dynamic coupling method for solids' transient calculations and fluids' steady-state calculations due to its promising accuracy and efficiency. Furthermore, they suggested that a relaxation parameter near the heat transfer coefficient offers advantages. Verstraete and Scholl [7] highlighted the Biot number's critical role in the coupling scheme's stability for conjugate heat transfer problems.

This paper focuses on a novel numerical method for coupling CFD and FEM in conjugated heat transfer, relevant for transient and steady-state analyses in aero engine and turbomachinery applications. The coupling involves utilizing a correlation function based on CFD data processed through an innovative artificial neural network approach. This correlation is applied at the boundary nodes of the FEM mesh to track the total deformation over time. The following Figure 1 shows the calculation scheme.

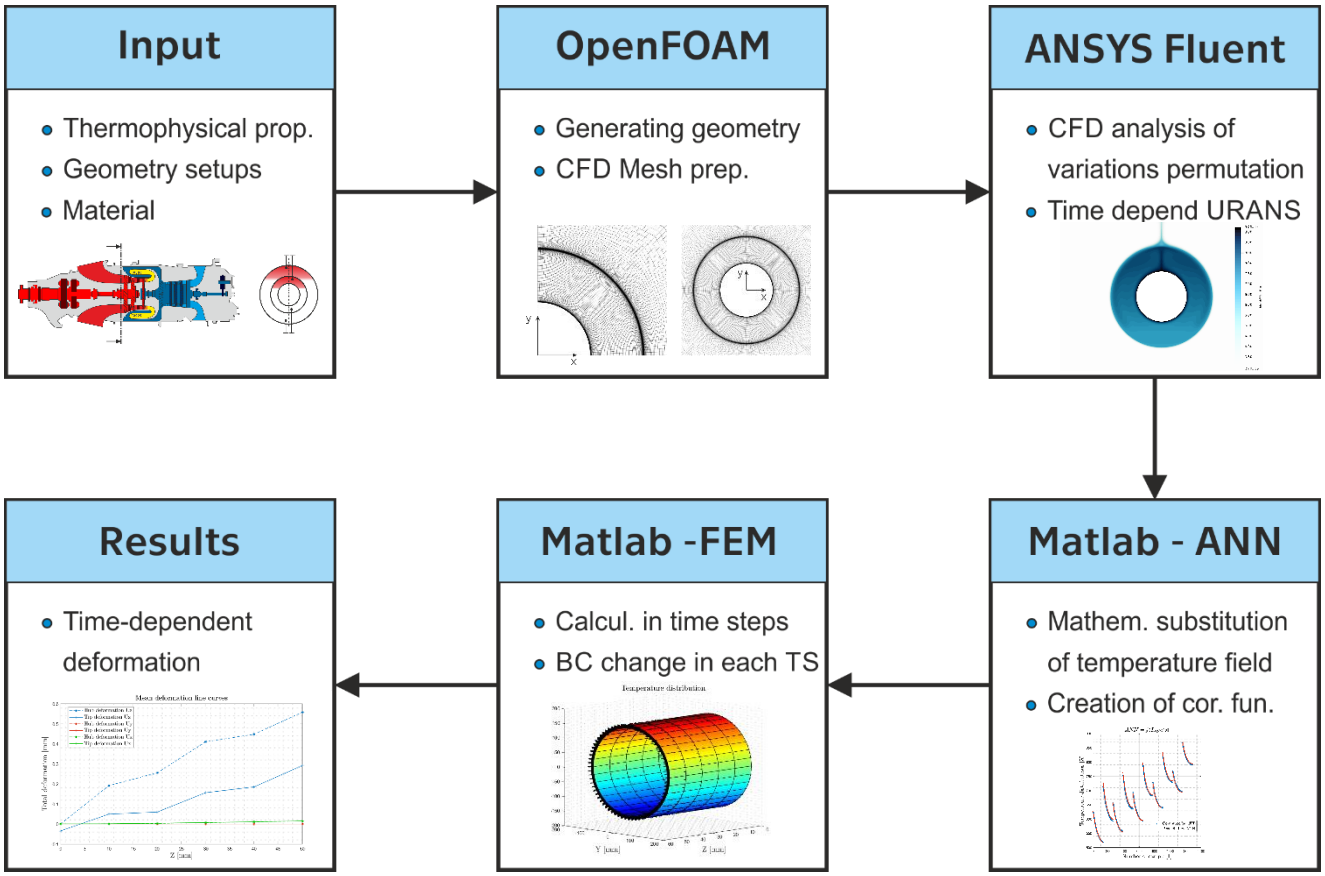

Figure 1 – CFD to FEM coupling using correlation function.

2. Objective Statement

2.1 Geometry

The scope assumed a single annular geometry, crucial in turbomachinery, specifically in compressor and turbine sections, as shown in Figure 2. This represents the flow path through the turbine engine. Specifically, the geometry is based on the turbine section of a turboprop engine.

The inner tube is a simplified wall of the gas flow path in the turbine section and outer tube represents the engine cowling. The annular space between these tubes is the free space in the engine.

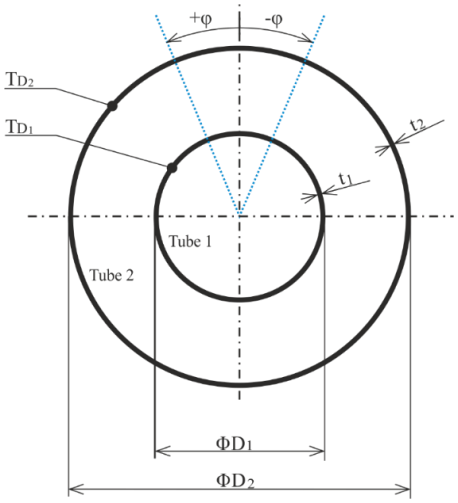

Figure 2 – Solved geometry scheme.

3. Complexity of the CFD Model

The initial conditions setup for the Computational Fluid Dynamics analysis are derived from the thermodynamic cycle specific to an aircraft engine operating in CRUISE flight mode, extensively discussed by Pařez et al. [8]. The temperature distribution across the outer tube is computed through CFD. This steady distribution of temperatures isn't uniform due to ongoing natural convection resulting from the steady, homogeneous heating of the inner tube, corresponding to the flow of hot gases through the turbine. Given that the outer tube emulates the gas turbine scenario, this temperature profile has a key role in determining the placement of electronic components or overall engine deformation, which can be calculated using the Finite Element Method.

The second transition case is similar to the first steady case, with the difference being the assumption of engine transient mode. This occurs when changing from one mode to another mode or after engine shutdown. If the engine is turned off, transient temperature distribution occurs based on the initial steady condition where the temperature field distribution is steady on the inner and outer tube. Thus, a non-stationary temperature field distribution from the first case is sought depending on the engine cooling parameters.

In the case of the transient calculation, the temperature field distribution over time was calculated after one second for several different settings from Table 1. The whole calculation was performed in Ansys Fluent. The meshing was performed in the BlockMesh program OpenFOAM package. The mesh itself is shown in Figure 3, where the refinement along the walls is shown. The URANS simulation setup includes a two-equation Generalised k-ω (GEKO) turbulence model [9].

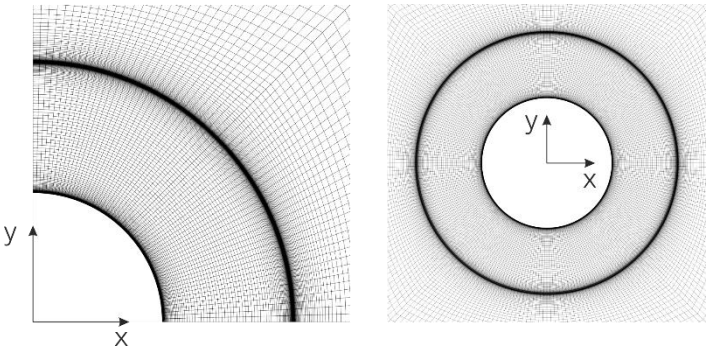

Figure 3 – Geometry mesh.

Heat radiation to the surfaces was considered as gray and diffuse surfaces. The heat exchange between these surfaces depends on factors such as their dimensions, separation distance, and orientation. Moreover, we consider processes like absorption, emission, and scattering of radiation. In this context, we implement the discrete ordinates (DO) radiation model [10].

The Boussinesq approximation with density effect on the temperature scale has been assumed for the reference pressure.

Table 1 – Input parameters for analysis.

Parameters	Unit	Variable
D_2	$[mm]$	(297)
D_1/D_2	$[1]$	$\{0.5, 0.6, 0.7, 0.8, 0.9\}$
T_{D1}	$[°C]$	$\{500, 600, 700\}$
t_2	$[mm]$	$\{1, 2, 3\}$
φ	$[°]$	$\{0, \dots, 360\}$

The Figure 4 below show the temperature and velocity distribution in a simple annular for the case D_1/D_2 = 0.5, t_2 = 1 [mm], T_{D1} = 700 [°C].

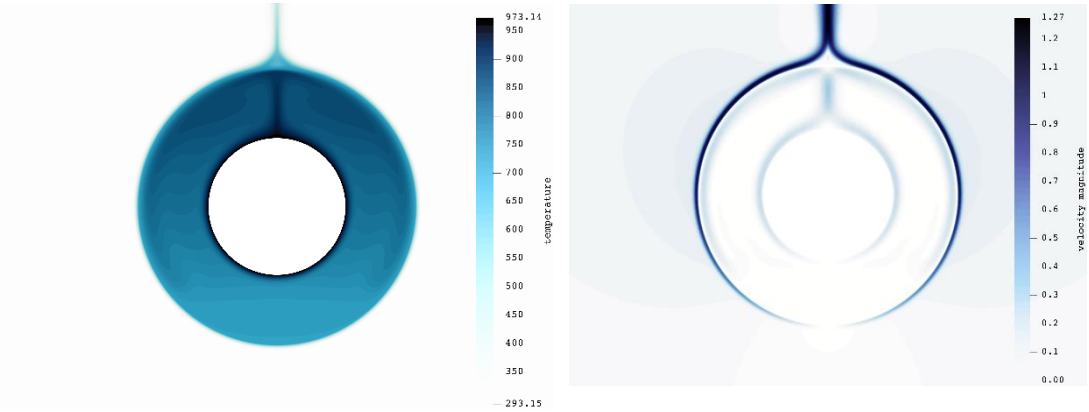

Figure 4 – Temperature and velocity field distribution for time = 0 [min].

4. Neural Network Approach

Mathematically, information processing within a neuron consists of two separate mathematical operations [11]. The first, the synaptic operation, includes the synapse weights, which represent the storage of knowledge, and thus memory of prior knowledge. The second is the somatic operation, which provides various mathematical operations such as thresholding, nonlinear activation, etc. The neural unit output $\tilde{y}$ is then scalar and is expressed by the following Equation 1.

$$\tilde{y} = \sigma(s). \tag{1}$$

Assuming an N-th order neural unit, then the product of the synaptic operation can be written as Equation 2.

$$s = w_0 x_0 + \sum_{i=1}^{n} w_i x_i + \sum_{i=1}^{n} \sum_{j=1}^{n} w_{ij} x_i x_j + \cdots$$
$$\sum_{i_1=1}^{n} \dots \sum_{i_N=i_N-1}^{n} w_{i_1 i_2 \dots i_n} x_{i_1} x_{i_2} \dots x_{i_n}, \tag{2}$$

where $x_0 = 1$ represents the threshold value and n represents the length of the input feature vector.

Since the desired outputs are predetermined, the process of machine learning is termed as supervised learning. This involves learning a function that connects input to output using a cost function $\vec{e}$. The output of a neuron is strongly dependent on the neuron's memories represented by a vector of weights $\vec{W}$. Thus, in order for a neural unit to learn, information processing must be appropriately structured. The batch Levenberg-Marquardt algorithm is used to update the weights [11].

$$\vec{W} = \vec{W} + \Delta\vec{W}, \tag{3}$$

where

$$\Delta\vec{W}^T = -\left(\vec{J}^T\vec{J} + \frac{1}{\mu}\vec{I}\right)^{-1}\vec{J}^T\,\vec{e}. \tag{4}$$

The coefficient μ is the learning rate, $\vec{I}$ is the $n_w \times n_w$ identity matrix, n_w the number of weights and $\vec{J}$ represents an $n \times n_w$ Jacobian matrix.

The correlation function is then obtained using an extensive set of CFD simulations shown for initial steady temperature distribution on Figure 5 and different operational conditions and geometrical setups shown on Figure 6.

A machine learning approach is applied to the CFD results and the only correlation function is obtained for a range of input variable parameters. A simplified notation of the correlation function is given below in Equation 5.

$$T_{D2} = f(T_{D1}, t_2, D_1/D_2, D_1). \tag{5}$$

To simplify the task, some assumptions have been made. First, the temperature is assumed to be symmetric along the vertical axis, and therefore the data with the corresponding angular coordinate are averaged. And secondly, due to the small temperature differences at the inner and outer edges of the outer tube and due to the error band resulting from the CFD discretization, it is assumed that the effect of the inner tube thickness can be neglected, so that the temperatures at these edges are also averaged.

The portion of the training data set that represents a single batch of D_1/D_2 ratios and T_{D1} boundary conditions prescribed on perturbations of the inner tube with a constant t_2 value is shown on Figure 6. Each data cluster represents one CFD simulation. As can be seen, the behavior is nonlinear, making it a suitable task for neural network learning.

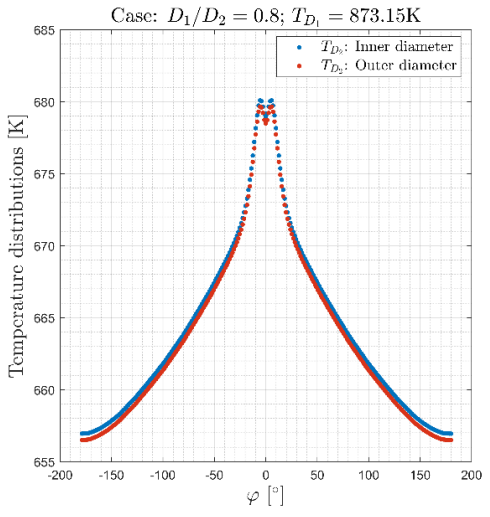

Figure 5 – Temperature distribution over the edges.

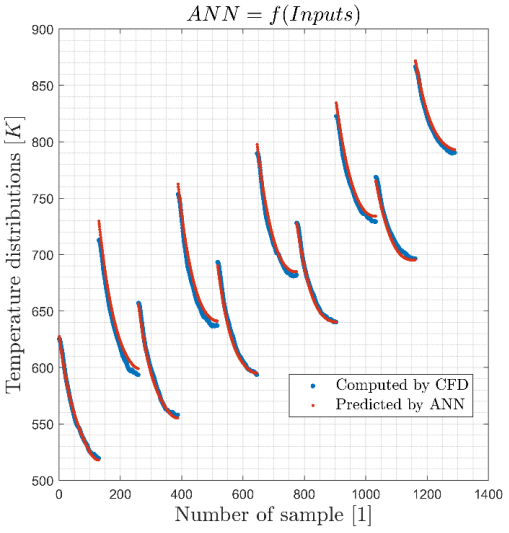

Figure 6 – Comparison of ANN and CFD data.

5. Boundary Conditions for FEM Solver

FEM software is commonly used to determine the strain and stress response to mechanical and thermal loads. The commonly used approach is to determine the temperature field distribution at the edge nodes of the geometry based on CFD flow calculations. Based on these initial conditions, material characterization and boundary conditions, the temperature field distribution is determined by the FEM calculation and finally the stress and deformation of the geometry is determined.

However, the CFD calculation is time consuming and in the case of non-stationary calculation there is a computational problem. Thus, it is desired to determine a nonstationary correlation function that can prescribe the temperature distribution for the edge nodes shown on the simple rotor geometry in Figure 7 and Figure 8. The geometry is discretized into a nodes mesh Figure 7, which is then built into an elements mesh as shown in Figure 8.

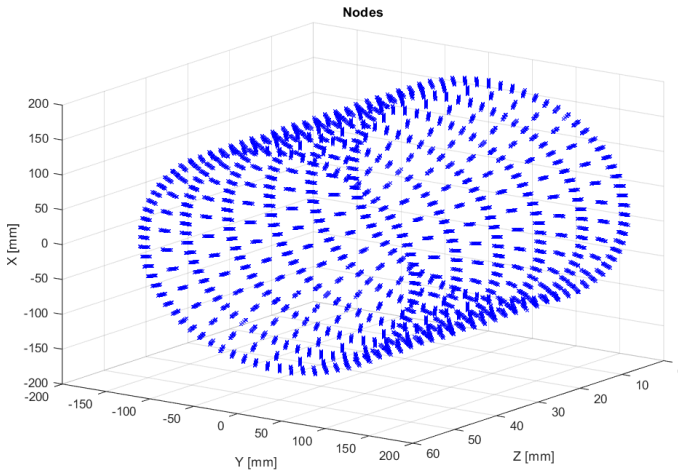

Figure 7 – Nodes mesh of simple geometry.

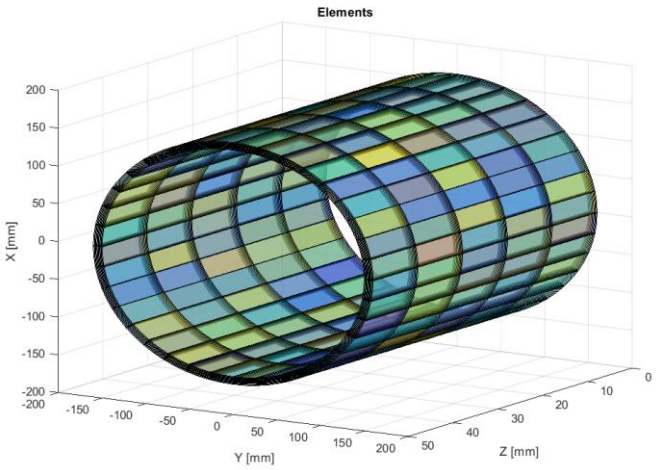

Figure 8 – Elements mesh of simple geometry.

The calculation is performed using the standard FEM calculation, which has been presented, for example, by Pařez and Kovář [12]. A computational tool was developed and based on the Matlab scripts, where the boundary condition prescription was written for the boundary nodes from Figure 7. These nodes have a prescribed boundary condition from Equation 5 to find the temperature as the parameters change over time and to find the temperatures for different changing geometry conditions.

The following Figure 9 shows the determined temperature field distribution based on the boundary temperatures. After the calculating of the temperature field, the deformation is calculated and shown by the strain vectors in Figure 9.

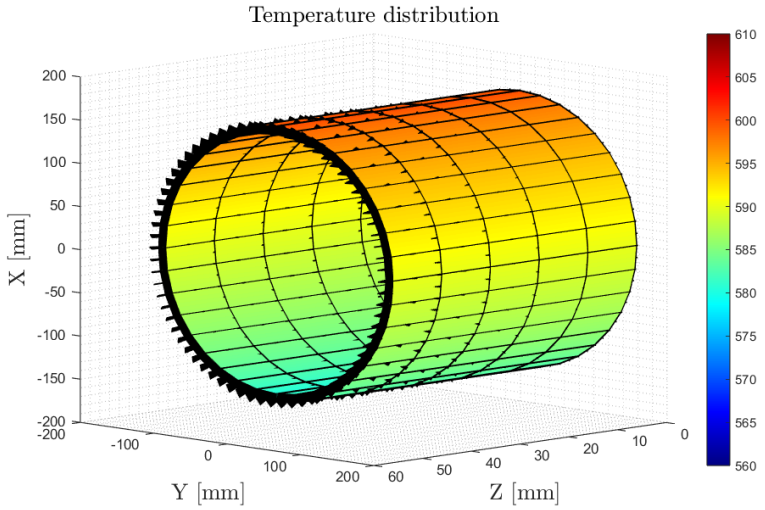

Figure 9 – Deformation for steady state mode - Cruise.

6. Improvement by Thermal Conductor

The calculation shows the effect of heat conduction in the tube, which leads to the idea of a thermal conductor. The following section studies the effect of increasing heat conduction by using thermal conductors. For simplicity, a bimetallic model was chosen in which the last layers of elements on the outer surface were prescribed a different material, namely copper C1020. The idea is that a coating would be applied to the surface of the geometry for better heat conduction.

The material characteristics are shown in the following Table 2.

Table 2 – Used materials.

Material	Young modulus	Poisson number	Thermal expansion Alpha	Conductivity
$[-]$	$[Pa]$	$[-]$	$[K^{-1}]$	$[W * m^{-1} * K^{-1}]$
$Steel$	$2.1e11$	0.3	$24.1e-6$	33
$Copper$	$1.20e11$	0.33	$17.7e-6$	391

From the deformation characteristics of two identical cases, the corresponding steady state calculation at 500 sec time with similarly defined boundary conditions are shown in Figures 10 and Figures 11. The temperature field distribution is improved due to the use of a temperature conductor on the surface. This also improves the deformation causing thermal bow.

This leads to the idea of improving and influencing the temperature field by means of temperature conductors implemented in the material and thus reducing the influence of natural convection in the case of transients and in the case of cooling of turbomachinery.

The deformations are shown in three directions Ux, Uy, Uz along the length of the annular tube Z. The Hub indicates the tube support and the Tip shows the deformation on the surface. There is a noticeable increase in deformation with increasing length, which is expected when the pipe is tightly supported.

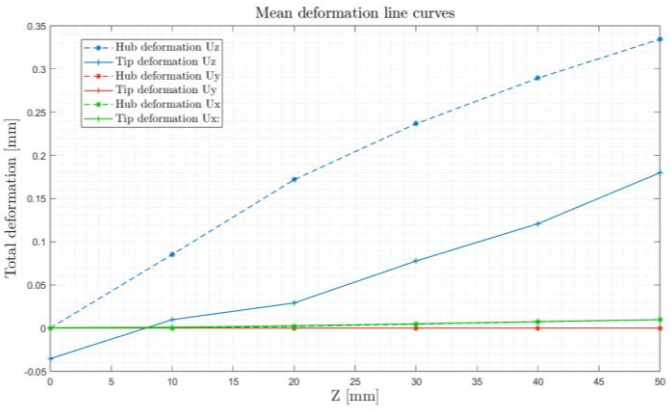

Figure 10 – Deformation for steady state mode with steel.

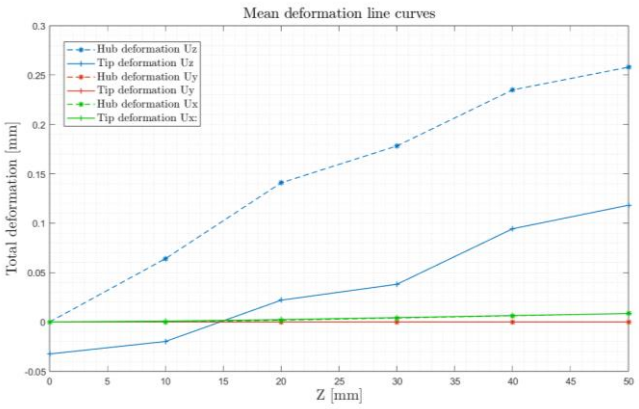

Figure 11 – Deformation for steady state mode with thermal conductor.

7. Results and Discussion

The nonstationary temperature-dependent deformation is shown in the following Figure 12 to Figure 15, which show represent the individual deformation and temperature time histories. On a simple annular tube, the temperature difference between the top and bottom of the tube is up to 30 degrees Celsius which, together with the tube support, causes uneven deformation between the top and bottom. The time histories of the deformation are then plotted in Figure 16 and Figure 17.

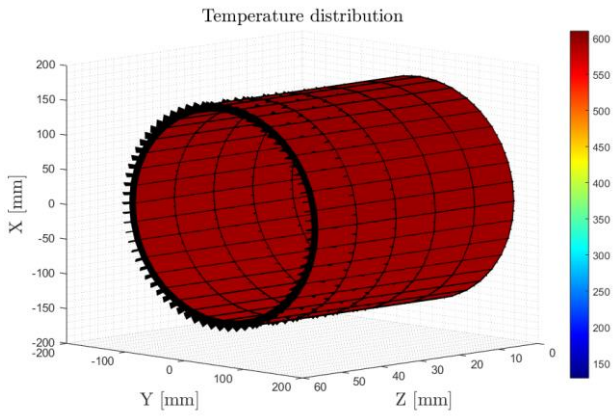

Figure 12 – Deformation initial 0 min.

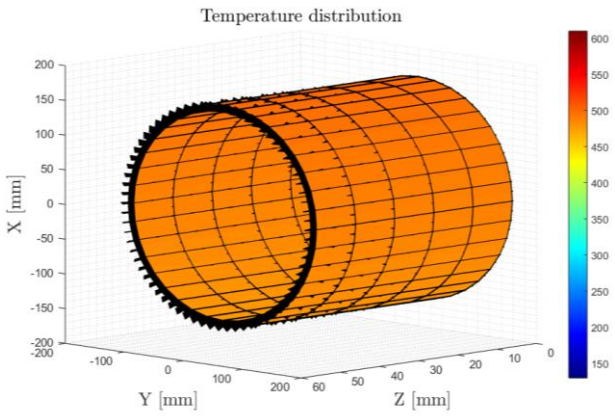

Figure 13 – Deformation after 8 min.

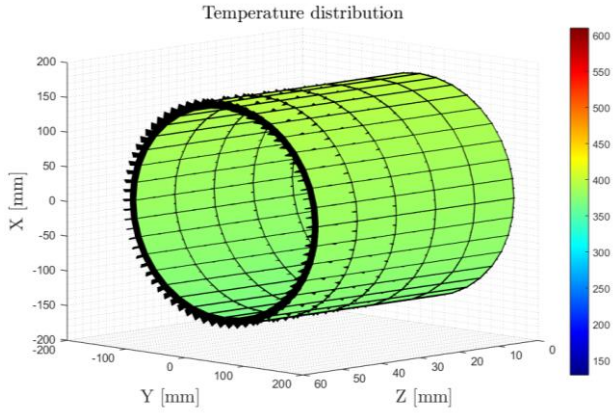

Figure 14 – Deformation after 16 min.

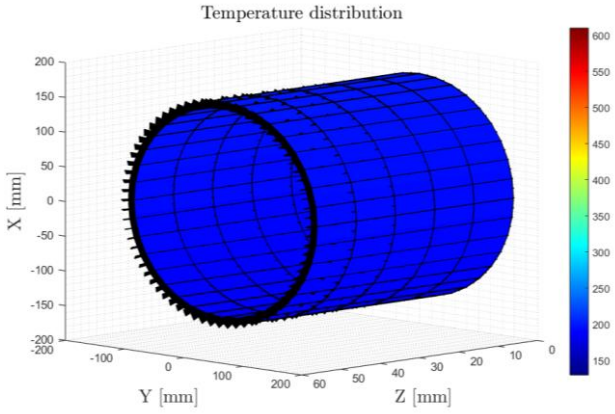

Figure 15 – Deformation after 25 min.

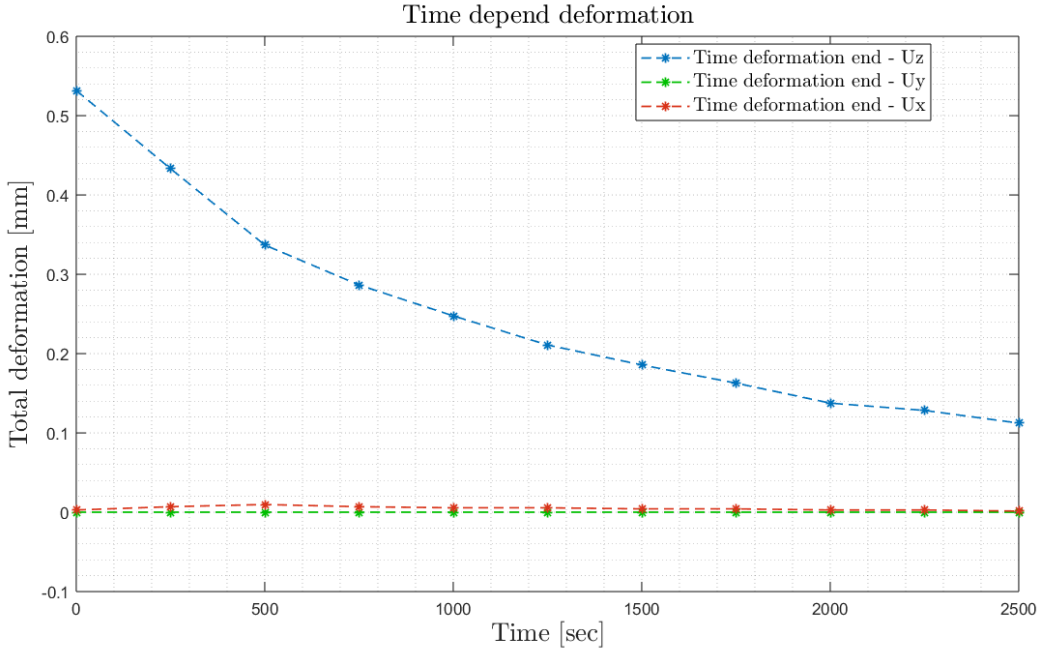

Figure 16 – Total deformation in time

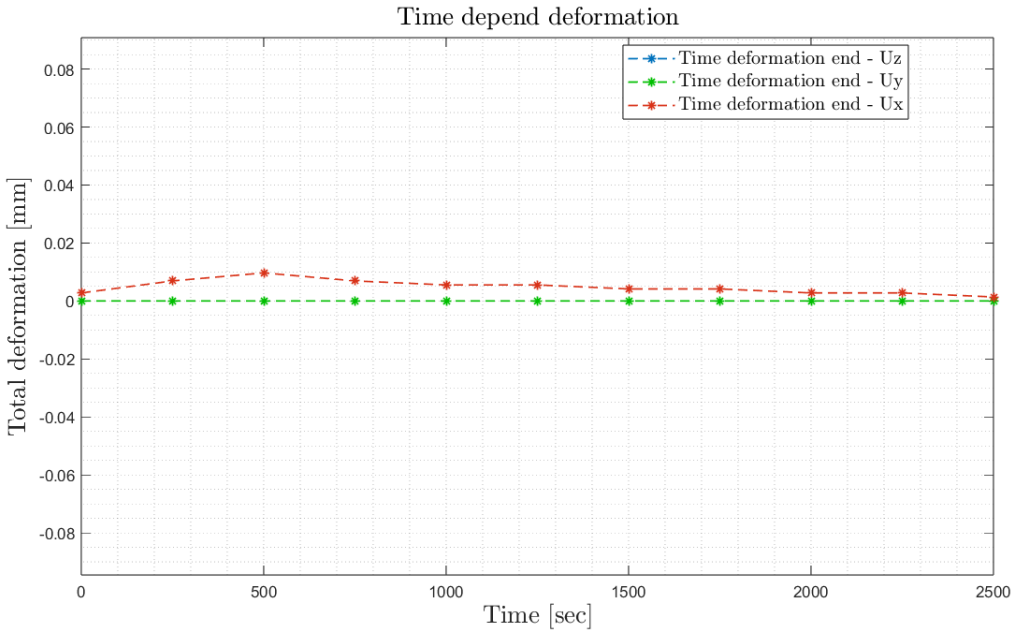

Figure 17 – Total deformation in time

8. Conclusion

This methodology allowed rapid estimation of temperature and strain distributions without the need for time-consuming CFD simulations. This significantly speeds up the design and development process, a critical factor in finite element transient analysis, where deformation is determined at each time step with time-dependent parameter variations. The objective was to determine a limited set of the most influential parameters affecting the temperature distribution of the outer tube. The values of the dependent parameters are given in Table 1.

The influential angular position parameter φ is assumed to be uniformly distributed around the pipe wall. The chosen parameters are only a simplification for the presented model. The number of inputs can be considered arbitrary with respect to the complexity of the computational model.

Based on the variation of these inputs, a CFD analysis of URANS is automatically computed as a starting point for machine learning.

The presented solution allows a new possible use of a machine learning procedure to determine a correlation function for strain prediction. From several computed CFD analyses, machine learning and mathematical dependencies can then be used to describe the behavior for any input in the computational range. By exploiting the prescription of the correlation function at the boundary points of the FEM network, a boundary condition for the finite element method calculation is given. At each time step, it is then possible to subtract the specified temperature and thus the time-varying strain. This is very advantageous as it simplify the calculation in order to reduce the time consumption.

The results have significant implications for the aerospace industry, particularly in optimizing the cooling of engine components. This methodology can enhance the design and manufacturing processes for turbines and compressors, leading to more efficient and reliable engines. The findings can be applied in practice for maintenance and condition monitoring of aircraft engines, potentially leading to more predictive maintenance strategies and improved engine performance. There is also potential for commercializing the methodology and integrating it into existing engine design software tools.

9. Acknowledgment

Authors acknowledge support from the ESIF, EU Operational Programme Research, Development and Education, and from the Center of Advanced Aerospace Technology (CZ.02.1.01/0.0/0.0/16_019/0000826), Faculty of Mechanical Engineering, Czech Technical University in Prague.

This work was supported by the Grant Agency of the Czech Technical University in Prague, grant No. SGS22/151/OHK2/3T/12.

10. Contact Author Email Address

The contact author is Jan Pařez, email address: Jan.Parez@fs.cvut.cz

11. Copyright Statement

References

[1] Perelman T. On conjugated problems of heat transfer. *Int. J. Heat Mass Transf.*, Vol. 3, pp 293–303, 1961.

[2] Fiedler B, Muller Y, Voigt M and Mailach R. Comparison of Two Methods for the Sensitivity Analysis of a One-Dimensional Cooling Flow Network of a High-Pressure-Turbine Blade. *In Volume 2D: Turbomachinery*; American Society of Mechanical Engineers: Vol. 1, New York, USA, 2020.

[3] Heselhaus A and Vogel D. Numerical simulation of turbine blade cooling with respect to blade heat conduction and inlet temperature profiles. *In Proceedings of the 31st Joint Propulsion Conference and Exhibit*, Vol. 1, San Diego, USA, 1995.

[4] Sun Z, Chew J W, Hills N J, Lewis L and Mabilat C. Coupled Aerothermomechanical Simulation for a Turbine Disk Through a Full Transient Cycle. *Journal of Turbomachinery*. Vol.134, No. 1, 2011.

[5] Errera M P and Duchaine F. Comparative study of coupling coefficients in Dirichlet–Robin procedure for fluid–structure aerothermal simulations. *J. of Computer Physics*, Vol. 312, No. 1, pp 218–234, 2016.

[6] Gimenez G, Errera, M P, Baillis D, Smith Y and Pardo F. A coupling numerical methodology for weakly transient conjugate heat transfer problems. *Int. J. Heat Mass Transf*. Vol. 97, No. 1, pp. 975–989, 2016.

[7] Verstraete T and Scholl S. Stability analysis of partitioned methods for predicting conjugate heat transfer. *Int. J. Heat Mass Transf*, Vol. 101, No.1, pp 852–869, 2016.

[8] Pařez J, Tater A, Kovář P, Polanský J and Vampola T. Investigation of temperature fields during turboprop engine cooling simplified to the 3D double annulus. *Proceedings of 15th European Conference on Turbomachinery Fluid dynamics & Thermodynamics.* The European Turbomachinery Society, 2023.

[9] Menter R F, Lechner R and Matyushenko A. *Best practice: generalized k-ω two-equation turbulence model in Ansys CFD (GEKO).* ANSYS, Germany, 2019.

[10] Chandrasekhar S. *Radiative transfer*. Dover Publications, 2013. ISBN 978-0-486-60590-6.

[11] Gupta M, Bukovsky I, Homma N and Hou Z G. Fundamentals of higher order neural networks for modeling and simulation. *Artificial Higher Order Neural Networks for Modeling and Simulation*, pp 103–133, 2013.

[12] Pařez J and Kovář P. Development and Application of a 3D FEM Model for Rotor Thermal Bow Prediction. *24th International Scientific Conference APPLIED MECHANICS 2023 BOOK OF ABSTRACTS*. Bratislava: Strojnícka fakulta STU v Bratislave, pp 93-96, ISBN 978-80-227-5294-7, 2023.